Mitigation of FOD and Corrosion Fatigue Damage in 17-4 PH Stainless Steel Compressor Blades with Surface Treatment

Paul S. Prevéy
Director of Research, Lambda Research, Cincinnati, OH 45227-3401
N. Jayaraman
Director of Materials Research, Lambda Research, Fair Lane, Cincinnati, OH 45227–3401
Ravi Ravindranath
NAVAIR, Patuxent River, MD 20670-1908

ABSTRACT

Compressor blades of a military aircraft turbine engine made of 17-4 PH stainless steel have been reported to have blade edge foreign object damage (FOD), corrosion pitting, and erosion damage that reduce fatigue life. This paper reports the findings of a comprehensive investigation of the effect of residual compressive stresses, imparted by various surface treatments, to improve leading edge damage tolerance and active corrosion fatigue performance in a salt water environment. Initial fatigue and corrosion fatigue tests were conducted in feature specimens designed to simulate the geometrical conditions of thick section and blade leading edges of compressor blades. The FOD tolerance and corrosion fatigue performance of 17-4PH prepared by low plasticity burnishing (LPB), shot peening (SP), and low stress grinding (LSG) were compared. LPB dramatically improved both high cycle fatigue (HCF) and corrosion fatigue performance, providing tolerance of 0.040 in. deep FOD in thick section and 0.050 in. deep leading edge FOD. Shot peening afforded little benefit in the presence of FOD 0.010 in. deep. Fatigue initiation at relatively low applied stress levels originating from existing corrosion pits outside of the LPB treated zone limited the ability to test the surface treatments on actual fielded T56 blades retired from service. In the absence of prior pitting, LPB provided 0.020 in. deep FOD tolerance on new T56 blades. Both the damage tolerance and active corrosion fatigue performance of 17-4PH in salt water increased with the depth of the compressive zone produced.

INTRODUCTION

Introduction of residual compressive stresses in metallic components has long been recognized[1-4] to lead to enhanced fatigue strength. For example, many engineering components have been shot-peened or cold worked with fatigue strength enhancement as the primary objective or as a by-product of a surface hardening treatment like carburizing/nitriding, physical vapor deposition, etc. Over the last decade, other examples of the former type of treatment like LPB[5], laser shock peening (LSP)[6], and ultrasonic peening[7] have emerged. In all surface treatment processes, key benefits are obtained when deep compression is achieved with minimal cold work of the surface. All of these surface treatment methods have been shown to benefit fatigue prone engineering components to different degrees.

Corrosion fatigue damage, stress corrosion cracking (SCC), FOD, and erosion damage are generally recognized as significant degradation processes that affect naval aircraft turbine engine compressor components. Precipitation hardened martensitic stainless steels, including 17-4PH, are widely used in applications where a combination of high strength and resistance to corrosion is needed. Components made of precipitation hardened martensitic stainless steels are known to be prone to corrosion fatigue and SCC.[8-11] Early research on this topic focused on mitigating corrosion fatigue damage and SCC by altering alloy chemistry, controlling the microstructure effects through heat treatment, as well as the incorporation of various surface treatments.

LPB has been demonstrated to provide a deep surface layer of high magnitude compression in various aluminum, titanium, nickel based alloys and steels. The deep compressive residual stress state on the surface of these materials mitigates fatigue damage including FOD,[12-14] fretting fatigue damage,[15-16] and corrosion fatigue damage.[17-20] The LPB process can be performed on conventional CNC machine tools at costs and speeds comparable to conventional machining operations such as surface milling.

17-4PH stainless steel 1st stage compressor blades have blade edge FOD, corrosion pitting, and erosion damage which reduces fatigue life. This paper reports the findings of a comprehensive investigation of the effects of residual compressive stress, imparted by a variety of surface treatments, to withstand FOD and resist corrosion pitting and corrosion fatigue. The main goal of this research was to investigate the effect of a compressive surface residual stress state imparted by surface treatment upon the mechanisms of corrosion fatigue and FOD in 17-4 PH stainless steel.

## EXPERIMENTAL PROCEDURE

Material and Heat Treatment

17-4 PH Stainless Steel was procured in the form of 0.5 in (~12.7 mm) thick plates. Bars of nominal dimensions of 0.375 X 1.25 X 8 in. (9.5 X 31.75 X 203.2 mm) were initially machined. All of the bars were heat-treated to the H1100 condition: aged at 593 °C (1100 °F) for 4 hours, followed by air-cooling. The nominal composition and tensile properties of the heat-treated steel are as follows:

Chemical Composition: (weight%) C-0.040%, Nb-0.32%, Cr-15.35%, Cu-3.39%, Mn-0.69%, Mo-0.24%, Ni-4.24%, P-0.024%, S-0.006%, Si-0.63%, Ti-<0.01%, Bal-Fe.

0.2% Y.S. = 156 ksi (~1,075 MPa), UTS = 160 ksi (~1,100 MPa), Elong. = 16%, RA = 66.4%

HCF Specimen Processing

Thick section (TS) and blade edge (BE) feature specimens (Figures 1a and 1b) were finish machined from the heat-treated bars by LSG. FOD was simulated by electrical discharge machined (EDM) notches. A semi-elliptical surface notch of depth of a_o = 0.01 in. (0.25 mm) and surface length of $2c_o$ = 0.06 in. (1.5 mm) was introduced in some thick section specimens. Notches of different depths in the range of a_o = 0.020 in (0.5 mm) to 0.050 in (0.125 mm) were introduced on the blade edge specimens (see Figures 2a and 2b).
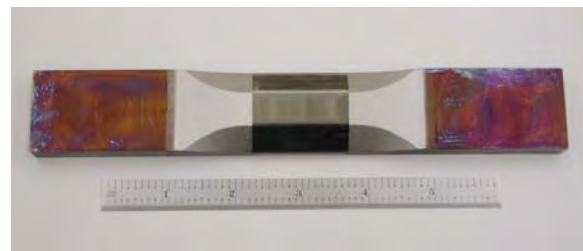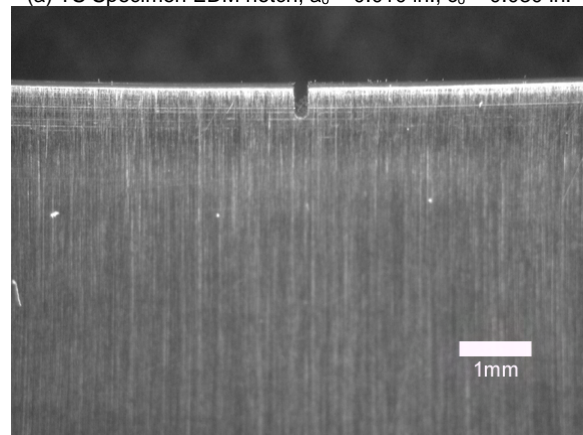

(a) Thick section specimen
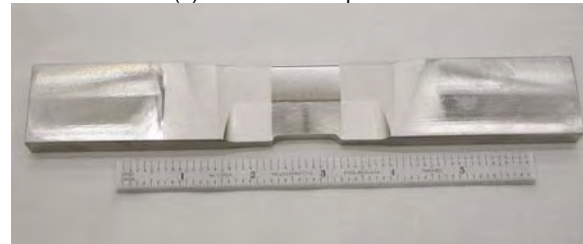
(b) Blade edge specimen

Figure 1 – Thick section and blade edge feature specimens.

(a) TS Specimen EDM notch, a_o = 0.010 in., c_o = 0.030 in.

1mm

(b) BE Specimen EDM notch, a_o = 0.020 in.

Figure 2 – EDM machined simulated FOD

Surface Treatment

LPB processing was performed using a single point tool for thick section specimens (Figure 3) and a caliper tool for blade edge specimens (Figure 4). The CNC control code was modified to allow positioning of the LPB tool in a series of passes along the gage section while controlling the burnishing pressure to develop the desired magnitude of compressive stress with relatively low cold working. Two sets of thick section specimens were shot peened using a conventional air blast peening system equipped with a rotating table with 125% coverage, 14CW shot and 8A Almen intensity.
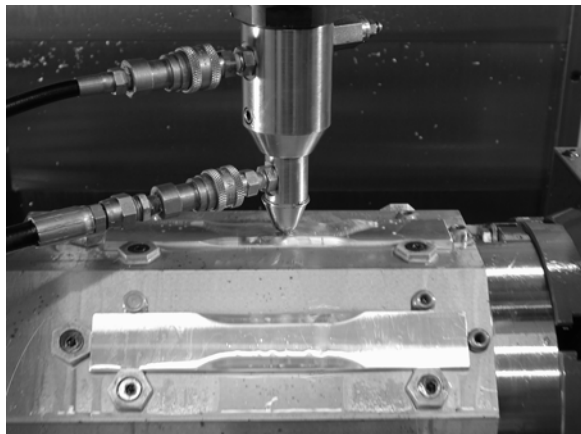

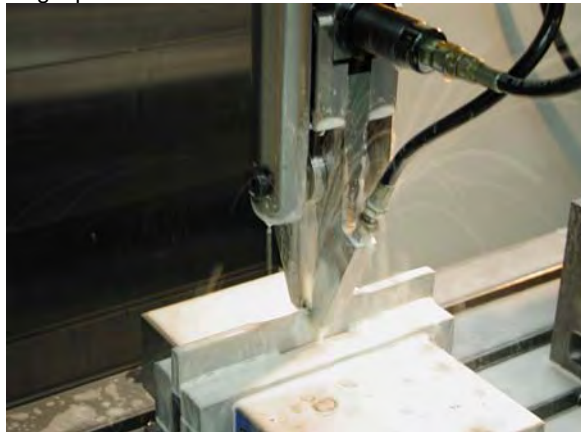Figure 3 – Surface treatment of TS specimen with single point tool.

Figure 4 – Surface treatment of BE specimen with caliper tool.

Residual Stress Measurement

X-ray diffraction residual stress measurements were made at the surface and at several depths below the surface on LPB treated fatigue specimens. Measurements were made in the longitudinal direction in the fatigue specimen gage employing a $\sin^2\psi$ technique and the diffraction of chromium Kα1 radiation from the (211) planes of steel. The lattice spacing was

first verified to be a linear function of $\sin^2\psi$ as required for the plane stress linear elastic residual stress model[21-24].

Material was removed electrolytically for subsurface measurement in order to minimize possible alteration of the subsurface residual stress distribution as a result of material removal. The residual stress measurements were corrected for both the penetration of the radiation into the subsurface stress gradient[24] and for stress relaxation caused by layer removal.[25]

The value of the x-ray elastic constants required to calculate the macroscopic residual stress from the strain normal to the (211) planes of steel were determined in accordance with ASTM E1426-9.[26] Systematic errors were monitored per ASTM specification E915.

High Cycle Corrosion Fatigue Testing

All high cycle fatigue tests were performed under constant amplitude loading on a Sonntag SF-1U fatigue machine. Fatigue testing was conducted at ambient temperature (~72F) in four-point bending mode at a cyclic frequency of 30 Hz and load ratio, R = 0.1. Corrosion fatigue tests were performed with the sample gage section exposed to a 3.5% NaCl salt solution at a pH of 7 (adjusted by adding either NaOH or HCL). Chemical-free tissues were soaked with the salt solution, taped to the gage section of the fatigue test specimen, and sealed with a plastic film to avoid evaporation. Table I lists the test matrix. Following fatigue testing, each specimen was examined optically at magnifications up to 60x to identify fatigue origins and locations thereof relative to the specimen geometry. Fractographs were taken with a Nikon 990 digital camera through a Nikon Stereoscopic microscope at 15x. A representative photograph of a typical failure for each specimen group was obtained. A few selected specimens were also examined under a Cambridge S90B SEM.

RESULTS AND DISCUSSION

Residual Stress Distributions

Residual stress distributions are presented graphically in Figures 5a and b. LSG produced surface compression of nominally -85 ksi (-585 MPa), which decreases rapidly to nearly zero at a depth of 0.002 in (0.05 mm), with 15% cold work on the surface. Surface compression from SP

was nominally -105 ksi (-725 MPa), becoming more compressive to nominally –125 ksi (-860 MPa) at a depth of 0.002 in (0.05 mm), and rapidly dropping to nearly zero residual stress at a depth of about 0.010 in (0.25 mm). SP produces nearly 70% cold work on the surface, which decreases to nearly zero within a depth of 0.005 in (0.125 mm). In contrast, LPB treatment produces surface compression of -100 ksi (-690 MPa), maximum compression to nominally -115 ksi (-790 MPa) at 0.005 in (0.125 mm), and gradually decreases to zero at a depth of about 0.040 in (1 mm). LPB produces surface cold work of less than 5%, which decreases to nearly zero within 0.001 in (0.025 mm).

TABLE I
Corrosion Fatigue Test Matrix

	LSG (Baseline)	LSG + Corrosion	LSG + FOD	LSG + FOD + Corrosion
hick Section Specimens	SP		SP + FOD	
	LPB	LPB + Corrosion	LPB + FOD	LPB + FOD + Corrosion
	All FOD 0.010 in. (0.25 mm deep)			
Blade Edge Specimens	LSG (Baseline)	LSG + Corrosion	LSG + FOD	LSG + FOD + Corrosion
	All FOD 0.020 in (0.5 mm deep)			
	LPB	LPB + Corrosion	LPB + FOD	LPB + FOD + Corrosion
	All FOD 0.020 in (0.5 mm) to 0.050 in (1.27 mm deep)			

In the LPB treated blade edge feature specimen (Figure 5b), the surface is compressive at nominally –75 ksi (-517 MPa). At depths of 0.005 and 0.014 in (0.12 and 0.36 mm) from the surface, the blade edge is in compression at –115 ksi (-793 MPa) and 85 ksi (586 MPa), respectively, indicating that through-thickness compression has been achieved back nominally 0.2 in (5 mm) chord wise from the leading edge. The equilibrating tension behind the compressive edge reaches a modest maximum of 25 ksi (172 MPa) at a distance of 0.25 in (6.3 mm) from the edge. Both the general compressive stresses and cold work seen on the surface of this specimen are attributed to the machining operation prior to LPB treatment. The low cold work associated with the LPB process is credited with the high stability of the compressive residual stresses of LPB treated parts to thermal exposure and mechanical overload conditions. In contrast, the SP treated specimens tend to go through recovery and recrystallization processes that are dominant in highly cold worked parts, and thereby lose the beneficial compressive residual stresses.

HCF and Corrosion Fatigue Performance of Thick Section Feature Specimens

Figures 6a - d show the HCF and corrosion fatigue performance of the thick section specimen in the form of S-N curves. In Figure 6a, the unnotched LSG condition has a fatigue strength, (endurance limit at about 10^7 cycles) S_{max} of nominally 150 ksi (~1035 MPa). In comparison, active corrosion fatigue of the LSG surface with exposure to 3.5% NaCl solution results in a fatigue strength of about 100 ksi (~690 MPa). Introduction of a semi-elliptical EDM notch of nominal size $a_o = 0.010$ in (0.25 mm) and $c_o = 0.030$ in (0.75 mm) drastically decreases the fatigue strength to about 20 ksi (140 MPa) for both air and corrosion environments. Power law lines were fitted to the data and are used in Figures 6b and c for purposes of comparison with other surface treatment processes.

In Figure 6b, the benefits of surface compression from the shot peening treatment are clearly seen by way of considerably improved HCF performance of the unnotched specimens, with a fatigue strength comparable to unnotched LSG (baseline) material. Introduction of a 0.010 in. (0.25 mm) deep notch reduces the endurance limit to be similar to the notched LSG (baseline) condition, a result expected given the depth of the corresponding residual stress profile (shown in Figure 5a) indicates a depth of compression much shallower than the depth the EDM notch.

In Figure 6c, the unnotched LPB treatment is shown to give a superior HCF performance with a fatigue strength of 190 ksi (1310 MPa). Also the fatigue data from all other tests (with FOD and/or corrosion) with LPB treatment may be grouped into one set of data, with corresponding fatigue strength of 140 ksi (965 MPa), comparable to the baseline fatigue strength. The deep compression with low cold working produced by LPB is seen to effectively mitigate the effects of both FOD and active salt-water corrosion fatigue.

Figure 6d summarizes the HCF and corrosion fatigue strength performance of the surface treatments for EDM notches up to a depth of 0.040 in. (1 mm). For both shot peened and LSG materials, even a 0.010 in. (0.25 mm) deep EDM notch greatly decreases the HCF and corrosion fatigue strength to a value between 25 and 40 ksi (170 and 275 MPa). In contrast, the LPB treated specimens withstand even a 0.040 in. (1 mm) deep EDM notch with a fatigue strength of

at least 55 ksi (380 MPa). The HCF and corrosion fatigue performance for the LPB treated specimens are easily explained based on the residual stress distributions seen in Figure 5a.
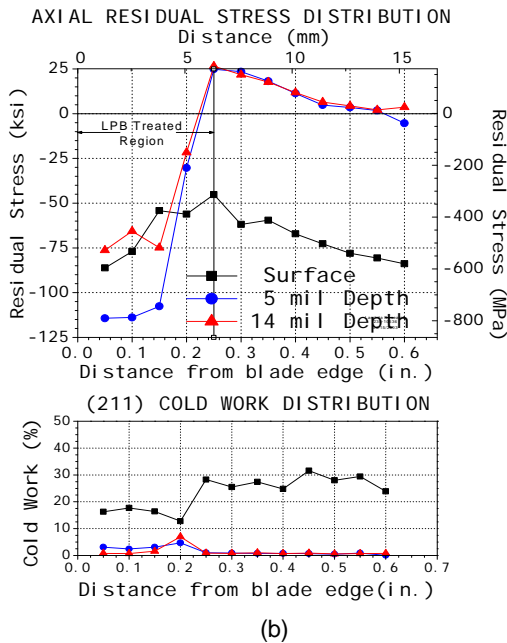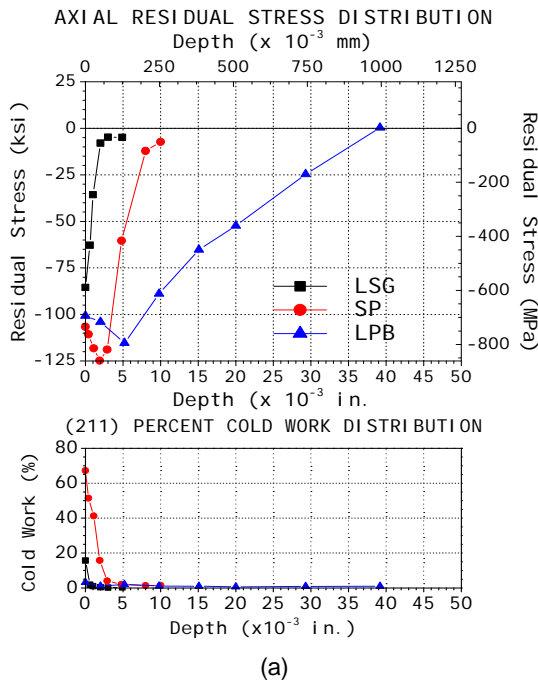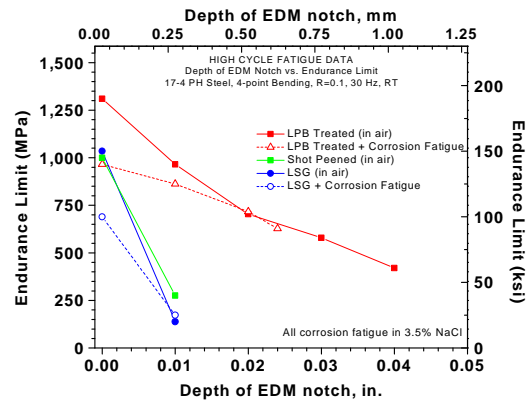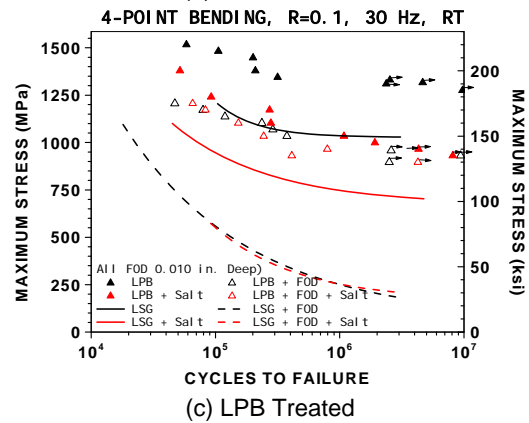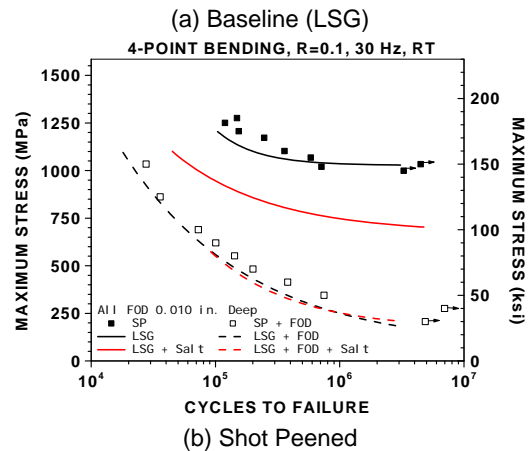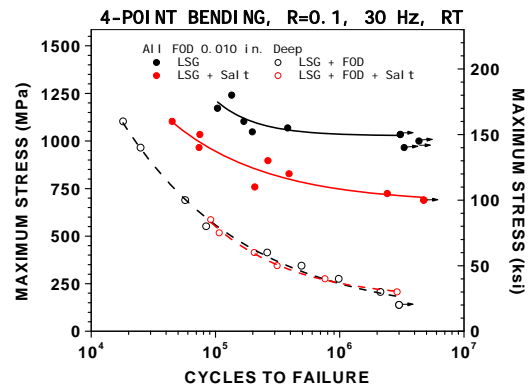

(a)

(b)

Figure 5 - Subsurface residual stress and cold work distributions for (a) LSG, SP and LPB processed thick section specimens, and (b) LPB processed blade edge simulation feature specimen

(a) Baseline (LSG)

(b) Shot Peened

(c) LPB Treated

(d)) Effect of notch depth on endurance limit

Figure 6 - HCF and Corrosion Fatigue data for 17-4PH thick section samples with surface treatments.

The general features of the fracture surfaces of samples tested in 3.5% NaCl solution (Figures 7a and b) are typical of corrosion assisted crack initiation, followed by fatigue crack growth to failure. Intergranular cracking attributed to stress corrosion cracking is evident at the initiation sites in both LSG and LPB treated specimens.
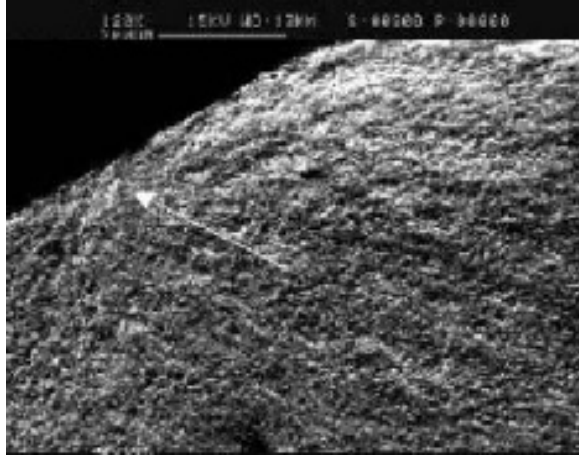
(a)

(b)

Figure 7 - SEM fractographs of corrosion fatigue tested Thick Section specimens – (a) LSG, Smax = 120 ksi (825 MPa), Nf = 391,342 cycles, (b) LPB, Smax = 150 ksi (1,035 MPa), Nf = 316,613 cycles – arrows indicate initiation

HCF and Corrosion Fatigue Performance of Blade Edge Feature Specimens

In Figure 8, the baseline HCF behavior of blade edge feature specimens have a fatigue strength of 170 ksi (1172 MPa), comparable to thick section feature specimens. Again, active corrosion has adverse effects on HCF behavior, decreasing the fatigue strength to 140 ksi (965 MPa). The additional effect of a 0.020 in (0.5

mm) deep EDM notch, with or without active corrosion is devastating, and reduces the fatigue strength to less than 10 ksi (70 MPa). Figure 9 shows that the LPB surface treatment completely mitigates the adverse effects of FOD and active corrosion. As in the case of thick section specimens, all LPB data fall into a narrow band, with a fatigue strength of 140 to 175 ksi (965 to 1206 MPa), independent of FOD or corrosion conditions. Figure 10 summarizes the fatigue performance of the blade-edge feature samples as a function of FOD depth. Fractographically, all LSG specimens had crack initiation in the gage section along the blade edge similar to Figure 11a, while most LPB specimens showed crack initiation sites close to the edge of LPB treatment below the blade edge, similar to Figure 11b. In the case of LPB, neither corrosion nor FOD had a significant impact on the fracture initiation stress and mechanisms.
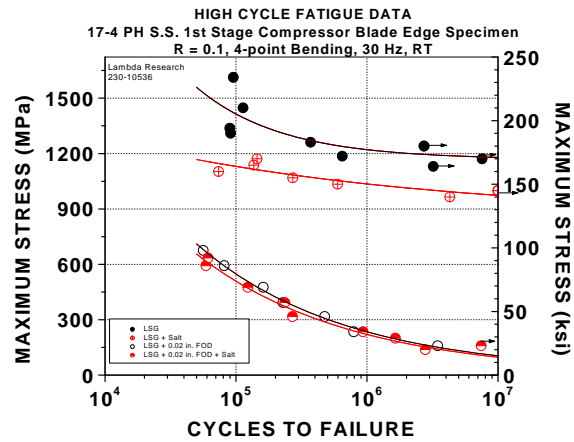

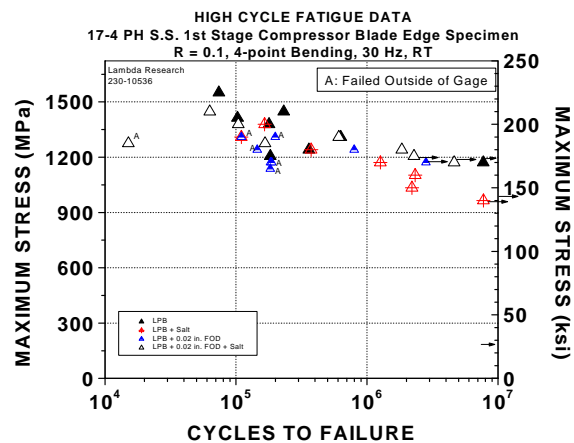Figure 8 – S-N curve for LSP blade edge simulation feature specimen.

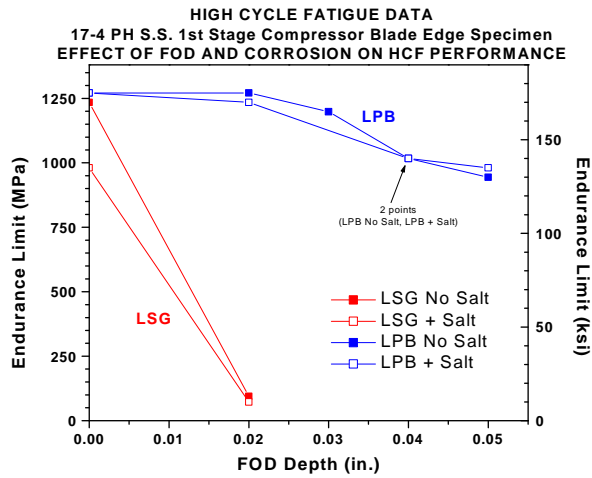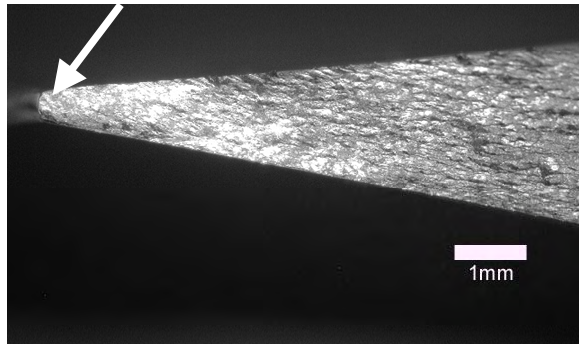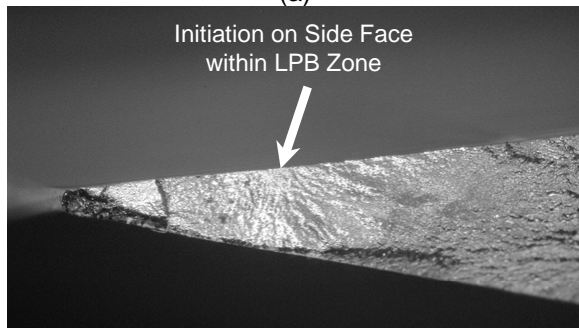Figure 9 – S-N curve for LPB blade edge simulation feature specimen.

Figure 10 - Effect of FOD depth and corrosion on HCF performance of blade edge specimens.

(a)

(b)

Figure 11 - (a) LSG + Salt Smax=155 ksi, Nf=271,494, (b) LPB + FOD + Salt Smax=200 ksi, Nf=165,274

HCF Performance of 1st Stage Compressor Blades

Several 17-4Ph 1st stage compressor blades retired from service for different reasons were acquired for testing. These blades were deemed unsuitable for service due to corrosion pitting, FOD, or erosion. Detailed damage characterization was performed on randomly selected blades from each group. A plot of the

size and distribution of damage in a typical blade is shown in Figure 12. A test program was developed to impart through-thickness compression to the lower third of the leading edge to improve FOD tolerance. With this goal, LPB processing of the leading edge (Figures 13a and b) resulted in compressive residual stresses shown in Figure 14.
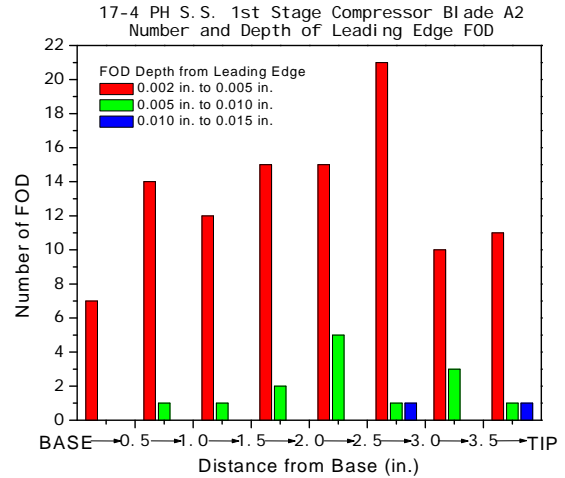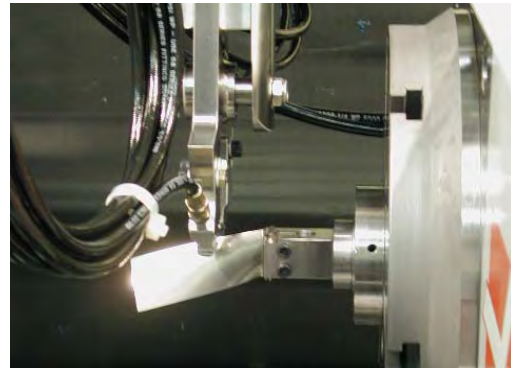

Figure 12 - Distribution of damage in a typical blade removed from service.

(a)

(b)

Figure 13 - (a) LPB processing of the leading edge, (b) the resulting LPB patch (holes near the blade tip are for loading the blades in the HCF test fixture).

9th National Turbine Engine High Cycle Fatigue Conference   7

Fatigue testing was performed in cantilever bending at 30 Hz, and an R-ratio of 0.3 by fixing the base of the blade at one end and flexing the tip in either easy-bending (I_{min} orientation) or hard-bending (I_{max} orientation) mode. Figure 15 shows these fixture arrangements. Blades instrumented with strain gages were used to calibrate the applied load vs stress along the leading edge. Figures 16a and b show the fatigue test results. As seen in Figure 16a, the blades removed from service and fatigue tested as received in the I_{min} orientation showed a fatigue strength in the range of 60 to 90 ksi (413 to 620 MPa). The significant scatter in the data is attributed to the presence of numerous randomly distributed pit and FOD defects that served as fatigue initiation sites. Introduction of a 0.010 or 0.020 in (0.25 or 0.5 mm) deep EDM notch on the leading edge reduced the fatigue strength to nominally 40 ksi (276 MPa). LPB processed blades tested at 110 ksi (758 MPa) also showed significant scatter, with fatigue lives ranging from 300,000 to 3,000,000 cycles. Fatigue results from tests performed in the I_{max} orientation also showed similar scatter in the data. EDM notches in the LPB blades ranging from 0.020 to 0.100 in (0.5 to 2.5 mm) had very little effect on fatigue performance. All fielded blades failed from corrosion pits or FOD from other regions of the blade. In the absence of prior corrosion pitting, LPB provided 0.020 in. deep FOD tolerance on new T56 blades.
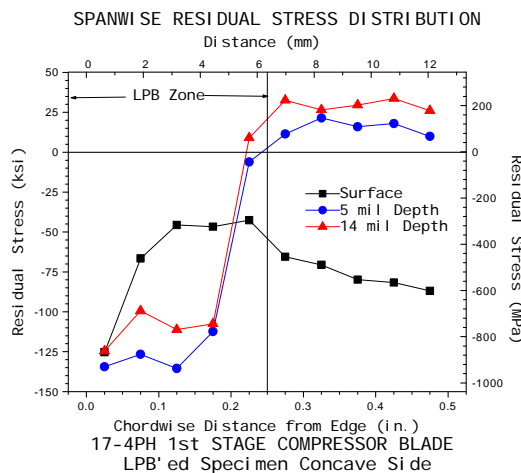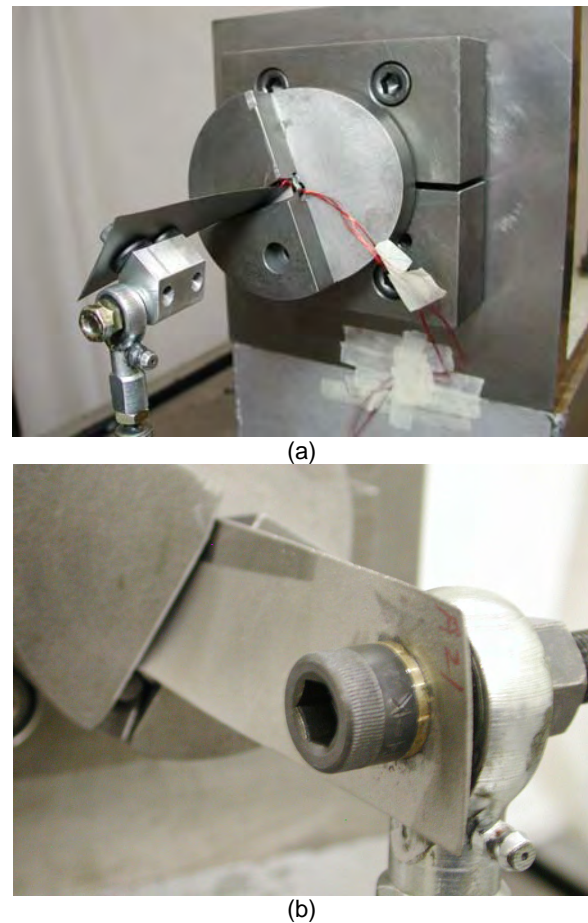

Figure 14 - Residual stress distributions produced at depths to mid-thickness.

Figure 17 shows the fractographs from a typical LPB treated blade with a 0.100 in (2.5 mm) EDM notch, where the crack initiated from an existing pit just outside the LPB patch, and final failure ensued. In general, these tests did not reveal

the true benefits of surface treatment because retired blades were rife with numerous corrosion pits damage in regions both in and outside of the surface treated areas, resulting in failure originating in untreated locations where the applied stress was much lower.

(a)

(b)

Figure 15 - Fatigue test fixtures – (a) easy bending (I_{min}), (a) hard bending (I_{max}) testing orientation
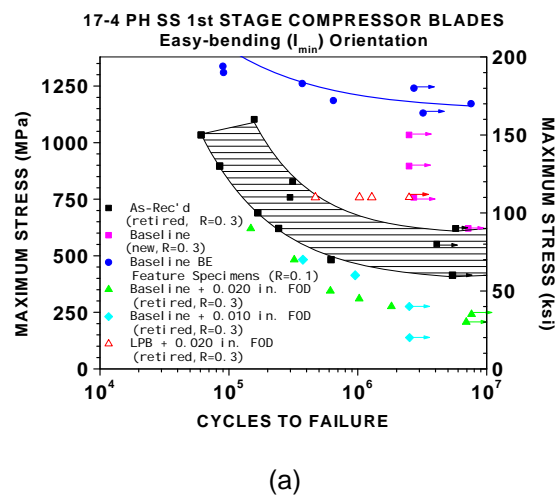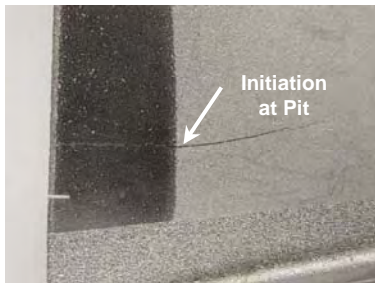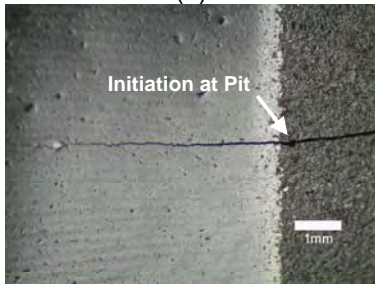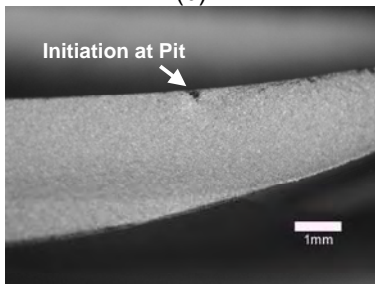

(a)
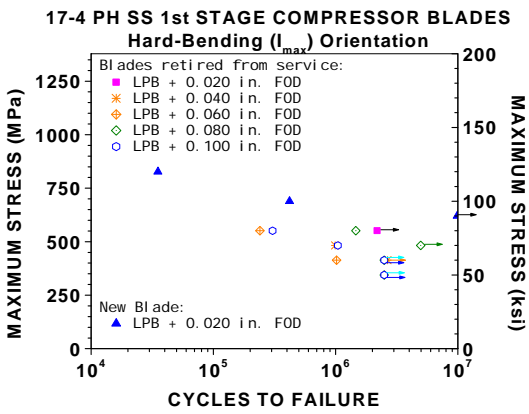
(b)

Figure 16 - Fatigue test results – (a) easy bending (I_{min}), (a) hard bending (I_{max}) testing orientation.

(a)

(b)

(c)

Figure 17 - LPB 1st Stage Compressor Blade with 0.100 in. FOD, showing failure initiation from a pit just outside of the LPB Zone - Smax=60 ksi, Nf=1,020,371.

SUMMARY AND CONCLUSIONS

The effects of surface treatment on the HCF strength, damage tolerance, and salt water corrosion fatigue behavior of 17-4 PH stainless steel used in the compressors of naval aircraft engines have been studied using both thick section and blade-edge feature specimens, and actual retired T56 1st stage compressor blades. Following are the conclusions from this study:

- Surface treatment with LPB of thick section surfaces of 17-4 PH stainless steel produces compressive residual stresses to a depth of 0.040 in (1mm) with little associated cold work. Shot peening produced a depth of compression of 0.010 in (0.25mm) with 70% cold work.
- LPB provided complete mitigation of both 0.010 in. deep FOD and active salt water corrosion fatigue. Assuming a Kt=3 design criteria, FOD up to 0.040 in. (1mm) deep was tolerated in thick sections.
- Through-thickness compression of nominally −100 ksi (-690 MPa) extending over 0.2 in. chord-wise from the leading edge was achieved by LPB processing of blade-edge feature specimens.
- Blade-edge FOD up to 0.050 in. deep in a salt-water environment was completely mitigated by LPB in feature samples.
- Because fielded T56 1st stage compressor blades failed prematurely from the existing corrosion pits, the effectiveness of surface treatment on actual blades could not be fully examined.
- In the absence of prior pitting, LPB provided 0.020 in. deep FOD tolerance on new T56 blades.

The improved damage tolerance is attributed to the high magnitude compressive residual stress delaying the initiation and early propagation of fatigue cracks from FOD. The fatigue debit associated with active salt-water corrosion fatigue is effectively mitigated by the high residual surface compression that maintains the stressed surface below the tensile threshold for corrosion fatigue.

ACKNOWLEDGEMENTS

and P. Mason for conducting fatigue tests and fractographic analysis.

REFERENCES

1. Frost, N.E. Marsh, K.J. Pook, L.P., *Metal Fatigue*, Oxford University Press, 1974.
2. Fuchs, H.O. and Stephens, R.I., *Metal Fatigue In Engineerin*g, John Wiley & Sons, 1980.
3. Berns, H. and Weber, L., "Influence of Residual Stresses on Crack Growth," Impact Surface Treatment, edited by S.A. Meguid, Elsevier, 33-44, 1984.
4. Ferreira, J.A.M., Boorrego, L.F.P., and Costa, J.D.M., "Effects of Surface Treatments on the Fatigue of Notched Bend Specimens," Fatigue, Fract. Engng. Mtrl., Struct., Vol. 19 No.1, pp 111-117,1996.
5. Prevéy, P.S. Telesman, J. Gabb, T. and Kantzos, P., "FOD Resistance and Fatigue Crack Arrest in Low Plasticity Burnished IN718", Proc of the 5th National High Cycle Fatigue Conference, Chandler, AZ. March 7-9, 2000.
6. Clauer, A.H., "Laser Shock Peening for Fatigue Resistance," Surface Performance of Titanium, J.K. Gregory, et al, Editors, TMS Warrendale, PA (1996), pp 217-230.
7. T. Watanabe, K. Hattori, et al, "Effect of Ultrasonic Shot Peening on Fatigue Strength of High Strength Steel," Proc. ICSP8, Garmisch-Partenkirchen, Germany, Ed. L. Wagner, pg 305-310.
8. F. J. Heyman, V. P. Swaminathan, J.W. Cunningham, "Steam Turbine Blades: Considerations in Design and a Survey of Blade Failure," EPRI Repot CS-1967, Palo Alto, CA, EPRI, 1981.
9. C.S. Carter, D.G. Warwick, A.M. Ross, J.M. Uchida, Corrosion, 27, 1971, p190.
10. R.M. Thompson, G.B. Kohut, D.R. Candfield, W.R. Bass, Corrosion, 47, 1991, p216.
11. V.P. Swaminathan, J.W. Cunningham, Corrosion Fatigue of Steam Turbine Blade Materials, ed., R.I. Jaffee, Pergamon Press, New York, NY, 1983, p.3.1
12. P. Prevéy, N. Jayaraman, R. Ravindranath, "Effect of Surface Treatments on HCF Performance and FOD Tolerance of a Ti-6Al-4V Vane," Proceedings 8th National Turbine Engine HCF Conference, Monterey, CA, April 14-16, 2003
13. Paul S. Prevéy, Doug Hornbach, Terry Jacobs, and Ravi Ravindranath, "Improved Damage Tolerance in Titanium Alloy Fan Blades with Low Plasticity Burnishing," Proceedings of the ASM IFHTSE Conference, Columbus, OH, Oct. 7-10, 2002
14. Paul S. Prevéy, et. al., "The Effect of Low Plasticity Burnishing (LPB) on the HCF Performance and FOD Resistance of Ti-6Al-4V," Proceedings: 6th National Turbine Engine High Cycle Fatigue (HCF) Conference, Jacksonville, FL, March 5-8, 2001.
15. M. Shepard, P. Prevéy, N. Jayaraman, "Effect of Surface Treatments on Fretting Fatigue Performance of Ti-6Al-4V," Proceedings 8th National Turbine Engine HCF Conference, Monterey, CA, April 14-16, 2003
16. Paul S. Prevéy and John T. Cammett, "Restoring Fatigue Performance of Corrosion Damaged AA7075-T6 and Fretting in 4340 Steel with Low Plasticity Burnishing," Proceedings 6th Joint FAA/DoD/NASA Aging Aircraft Conference, San Francisco, CA, Sept 16-19, 2002
17. N. Jayaraman, Paul S. Prevéy, Murray Mahoney, "Fatigue Life Improvement of an Aluminum Alloy FSW with Low Plasticity Burnishing," Proceedings 132nd TMS Annual Meeting, San Diego, CA, Mar. 2-6, 2003.
18. Paul S. Prevéy and John T. Cammett, "The Influence of Surface Enhancement by Low Plasticity Burnishing on the Corrosion Fatigue Performance of AA7075-T6," Proceedings 5th International Aircraft Corrosion Workshop, Solomons, Maryland, Aug. 20-23, 2002.
19. John T. Cammett and Paul S. Prevéy, "Fatigue Strength Restoration in Corrosion Pitted 4340 Alloy Steel Via Low Plasticity Burnishing." Retrieved from www.lambda-research.com Sept. 5, 2003.
20. Paul S. Prevéy, "Low Cost Corrosion Damage Mitigation and Improved Fatigue Performance of Low Plasticity Burnished 7075-T6", Proceedings of the 4th International Aircraft Corrosion Workshop, Solomons, MD, Aug. 22-25, 2000.
21. Hilley, M.E. ed.,(2003), <u>Residual Stress Measurement by X-Ray Diffraction</u>, HS*J784*, (Warrendale, PA: SAE).
22. Noyan, I.C. and Cohen, J.B., (1987) <u>Residual Stress Measurement by Diffraction and Interpretation</u>, (New York, NY: Springer-Verlag).
23. Cullity, B.D., (1978) <u>Elements of X-ray Diffraction</u>, 2nd ed., (Reading, MA: Addison-Wesley), pp. 447-476.
24. Prevéy, P.S., (1986), "X-Ray Diffraction Residual Stress Techniques," *Metals Handbook*, **10**, (Metals Park, OH: ASM), pp 380-392.
25. Koistinen, D.P. and Marburger, R.E., (1964), <u>Transactions of the ASM</u>, **67**.
26. Moore, M.G. and Evans, W.P., (1958) "Mathematical Correction for Stress in Removed Layers in X-Ray Diffraction Residual Stress Analysis," SAE Transactions, **66**, p p. 340-345.